Supplementary Information

for

Slow relaxation in $\{Tb_2Ba(\alpha\text{-fur})_8\}_n$ polymer with Ln=Tb(III) non-Kramers ion

E. Bartolomé, A. Arauzo, J. Luzón, S. Melnic, S. Shova, D. Prodius, J. Bartolomé, A. Amann,
M. Nallaiyan, S. Spagna

S1. Crystal structure of the {Tb_2Ba} polymer

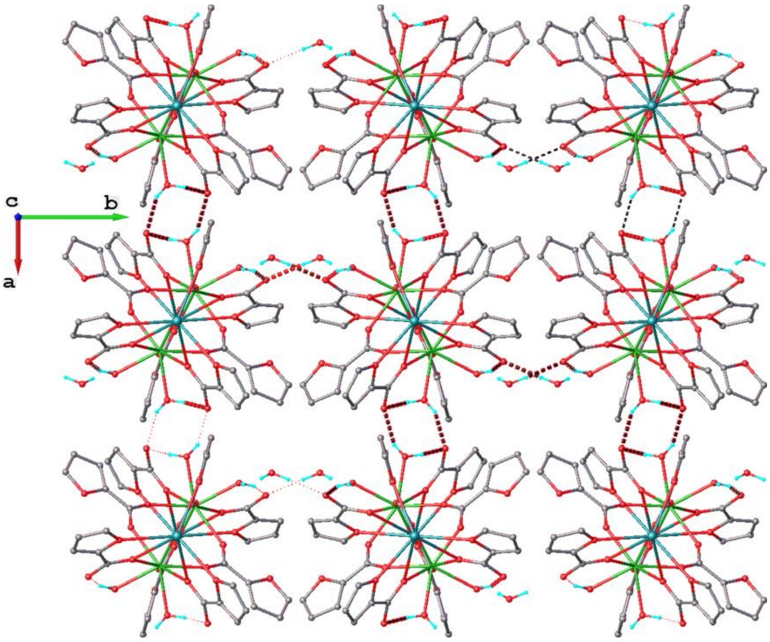

Fig. S1 3D supramolecular network formed by polymeric coordination chains.

Table S1. Selected bond distances for **(Tb_2Ba)**.

Tb1	O1^{2}	2.398(3)
Tb1	O1W	2.373(3)
Tb1	O2	2.306(3)
Tb1	O2W	2.408(3)
Tb1	O4	2.313(3)
Tb1	O5^{2}	2.349(3)
Tb1	O7	2.526(3)
Tb1	O10	2.464(3)
Ba1	O1	2.726(3)
Ba1	O1^{3}	2.726(3)
Ba1	O3	2.961(3)
Ba1	O3^{3}	2.961(3)
Ba1	O7^{2}	2.800(3)
Ba1	O7^{4}	2.800(3)
Ba1	O9^{2}	2.866(3)
Ba1	O9^{4}	2.866(3)
Ba1	O10^{4}	2.904(3)
Ba1	O10^{2}	2.904(3)
Ba1	O12^{2}	2.858(3)
Ba1	O12^{4}	2.858(3)

Symmetry code: ^{1}1 - *x*,1 - *y*,1 - *z*.

S2. *Ab initio* calculations

Levels	Energy (K)	|-6>	|-5>	|-4>	|-3>	|-2>	|-1>	|0>	|+1>	|+2>	|+3>	|+4>	|+5>	|+6>
$\|\xi_0\rangle$	0	**0.45**	0.00	**0.04**	0.00	0.01	0.00	0.00	0.00	0.01	0.00	**0.04**	0.00	**0.45**
$\|\xi_1\rangle$	3.22	**0.46**	0.00	**0.04**	0.00	0.00	0.00	0.00	0.00	0.00	0.00	**0.04**	0.00	**0.46**
$\|\xi_2\rangle$	119.94	0.00	0.36	0.00	0.10	0.00	0.04	0.00	0.04	0.00	0.10	0.00	0.36	0.00
$\|\xi_3\rangle$	133.60	0.00	0.42	0.00	0.07	0.00	0.00	0.00	0.00	0.00	0.07	0.00	0.42	0.00
$\|\xi_4\rangle$	12.24	0.04	0.00	0.23	0.00	0.15	0.00	0.16	0.00	0.15	0.00	0.23	0.00	0.04
$\|\xi_5\rangle$	270.28	0.04	0.00	0.39	0.00	0.05	0.01	0.00	0.01	0.05	0.00	0.39	0.00	0.04
$\|\xi_6\rangle$	294.03	0.00	0.10	0.00	0.19	0.02	0.19	0.00	0.19	0.02	0.19	0.00	0.10	0.00
$\|\xi_7\rangle$	302.55	0.00	0.01	0.04	0.08	0.21	0.02	0.26	0.02	0.21	0.08	0.04	0.01	0.00
$\|\xi_8\rangle$	306.04	0.00	0.04	0.01	0.10	0.09	0.26	0.00	0.26	0.09	0.10	0.01	0.04	0.00
$\|\xi_9\rangle$	435.25	0.00	0.05	0.01	0.22	0.02	0.20	0.00	0.20	0.02	0.22	0.01	0.05	0.00
$\|\xi_{10}\rangle$	428.03	0.01	0.00	0.16	0.02	0.09	0.00	0.44	0.00	0.09	0.02	0.16	0.00	0.01
$\|\xi_{11}\rangle$	511.49	0.00	0.01	0.07	0.00	0.36	0.00	0.13	0.00	0.36	0.00	0.07	0.01	0.00
$\|\xi_{12}\rangle$	511.97	0.00	0.01	0.01	0.21	0.00	0.27	0.00	0.27	0.00	0.21	0.01	0.01	0.00

Table S2 *Ab initio* calculated energy levels of the Tb single-ion, and eigenstates of Tb(III) in terms of the free ion wave functions. The numbers in the table indicate the weight of the $|+M_J\rangle$ and $|-M_J\rangle$ states.

Table S3 Seven first energy levels of the magnetic Tb$_2$ dimer, calculated with the parameters ZFS Δ_{Tb}/k_B=3.22 K, and intradimer interaction J^*/k_B=-1.12 x 10^{-2} K.

Levels	Energy (K)
$\|\varphi_0\rangle$	0
$\|\varphi_1\rangle$	2.58
$\|\varphi_2\rangle$	4.03
$\|\varphi_3\rangle$	6.60
$\|\varphi_4\rangle$	122.61
$\|\varphi_5\rangle$	122.88
$\|\varphi_6\rangle$	125.94
$\|\varphi_7\rangle$	125.97

Table S4 Composition of the four lowest dimer eigenstates, $|\varphi_i\rangle$, as a function of the ground and first states, $|\xi_0\rangle$ and $|\xi_1\rangle$, of the single-ions.

$|\varphi_0\rangle$=0.99 $|\xi_0\rangle|\xi_0\rangle$
$|\varphi_1\rangle$=0.71$|\xi_0\rangle|\xi_1\rangle$ - 0.71$|\xi_1\rangle|\xi_0\rangle$
$|\varphi_2\rangle$=0.71$|\xi_1\rangle|\xi_0\rangle$ - 0.71$|\xi_0\rangle|\xi_1\rangle$
$|\varphi_3\rangle$=0.99 $|\xi_1\rangle|\xi_1\rangle$

Table S5 Composition of the four lowest dimer eigenstates, $|\varphi_i\rangle$, as a function of the $|+M_J\rangle$ and $|-M_J\rangle$ states of the single-ions. The coefficients are expressed using module and phase.

$|\varphi_0\rangle$=0.44e$^{-0.59\pi i}$ |+6>|+6> + 0.46|+6>|-6> + 0.46|-6>|+6> + 0.44e$^{+0.73\pi i}$ |-6>|-6>
$|\varphi_1\rangle$= 0.64 |+6>|-6> - 0.64|-6>|+6>
$|\varphi_2\rangle$=0.64 |+6>|+6> + 0.64e$^{+0.32\pi i}$ |-6>|-6>
$|\varphi_3\rangle$=0.46e$^{-0.27\pi i}$ |+6>|+6> + 0.45|+6>|-6> + 0.45|-6>|+6> + 0.46e$^{+0.41\pi i}$ |-6>|-6>

The following dimer Hamiltonian has been used to model the **Tb_2Ba** system and fit the experimental *M*(*H*), χT and HC curves:

$$H_{dimer} = \sum_{i=1,2} H_{Tb,i} - 2J'\overrightarrow{J_1} \cdot \overrightarrow{J_2} + \sum_{i=1,2} g_J \mu_B \overrightarrow{J_\iota} \cdot \vec{H} + \sum_{i=1,2}(A\overrightarrow{J_\iota} \cdot \overrightarrow{I_\iota} - g_N \mu_B \overrightarrow{I_\iota} \cdot \vec{H}) \qquad [S1]$$

where $H_{Tb,i}$ is the electronic single-ion Hamiltonian producing the single-ion eigenstates and their corresponding energies. The second Hamiltonian term accounts for the intradimer magnetic interaction, the third one is the Zeeman term and the last is the hyperfine contribution and nuclear Zeeman term.

The complete single-ion wavefunction, including the nuclear wavefunction is constructed as the product J⊗I, J=6 and I=3/2, generating a complete base of 13x4=52 functions of the type:

$$|\xi_i, I_z\rangle = |\xi_i\rangle |I, I_z\rangle \qquad [S2]$$

The wavefunctions for the dimer are constructed as a product of the two monoatomic wavefunctions, indexed with subscript 1 and 2:

$$|\phi_k\rangle = \left|\xi_{i,1}, I_{z.1}\right\rangle \left|\xi_{ij,2}, I_{z.2}\right\rangle \qquad [S3]$$

The complete base has a dimension 52^2=2704.

Therefore it is convenient to perform the calculations for the very low temperature range, where the H_{hyp} becomes relevant, using a restricted electronic-nuclear base considering only the lowest energy monoatomic electronic eigenfunctions. In the case this confined Hamiltonian is expressed in a S*=1/2 formalism for the electronic wavefunction takes the following form:

$$H^*_{dimer} = \sum_{i=1,2} \Delta_{Tb} S^*_{i,x} - 2J'^* \, \vec{S}^*_{i,z} \cdot \vec{S}^*_{i,z} + \sum_{i=1,2} g^*_z \mu_B \vec{S}^*_{i,z} \cdot \vec{H} + \sum_{i=1,2}(A^* \vec{S}_i \cdot \vec{I}_i - g_N \mu_B \vec{I}_i \cdot \vec{H}) \qquad [S4]$$

Eq. S2 and Eq.S3 wavefunctions are restricted to i=0,1, and for the monoatomic wavefunctions base becomes 2x4=8 dimension, and 8^2=64 for the dimeric wavefunctions $|\phi^*_k\rangle$, where the * indicates the restriction to the S*=1/2 approximation. The total eigenfunctions obtained by diagonalizing H^*_{dimer} in this base are linear combinations of the 64 dimension restricted base $|\phi^*_k\rangle$ wavefunctions.

Below, the *electronic* energy level diagrams for a Tb_2 dimer as a function of a magnetic field applied along the EAM are shown, calculated for three different sets of values for the Δ_{Tb} and intradimer interaction J'^* for the sake of comparison. At H=0 the hyperfine interaction would produce further splittings.

a) Δ_{Tb}=3.22 K and J'^*=0

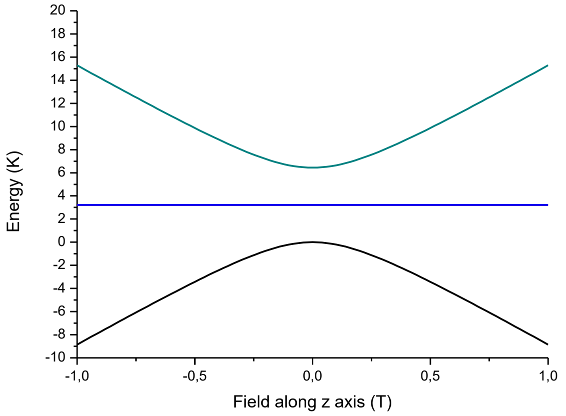

b) Δ_{Tb} =0 and J'^*=-1.6 K

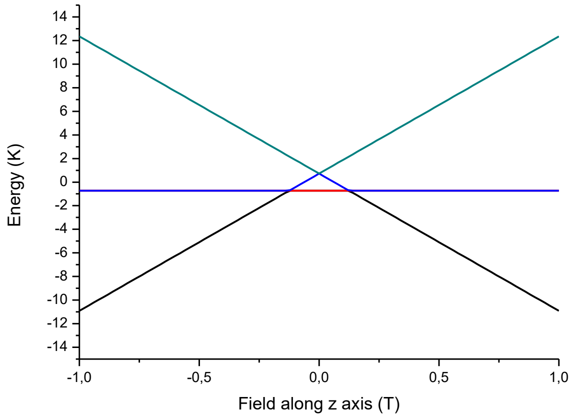

c) Δ_{Tb} =3.22 K and J'^*=-1.6 K

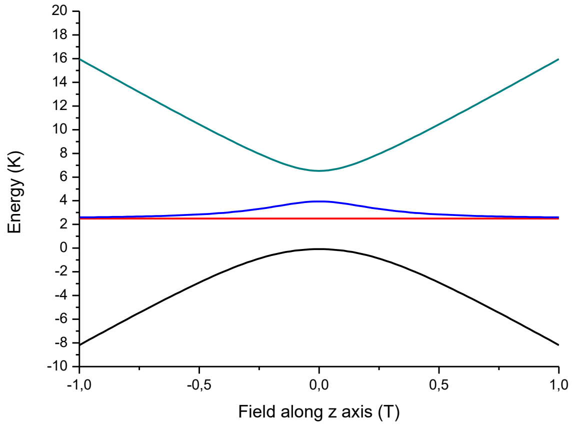

S3. Heat Capacity measurements

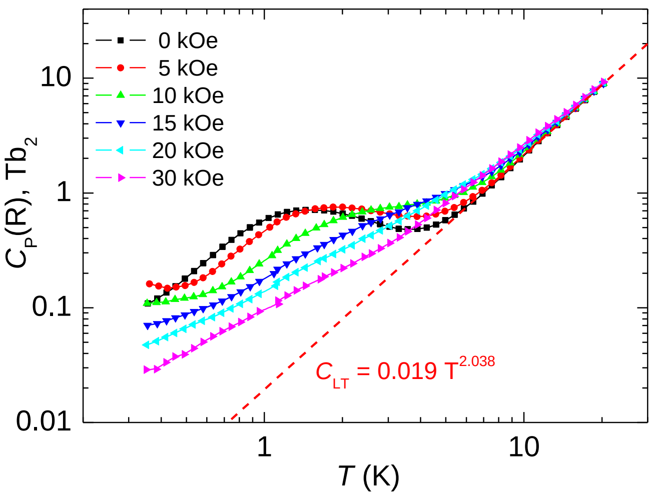

Fig. S2 Heat capacity at H=0 and different applied field up to H=30 kOe. Dashed line: estimated lattice contribution.

S4. Susceptibility modelization

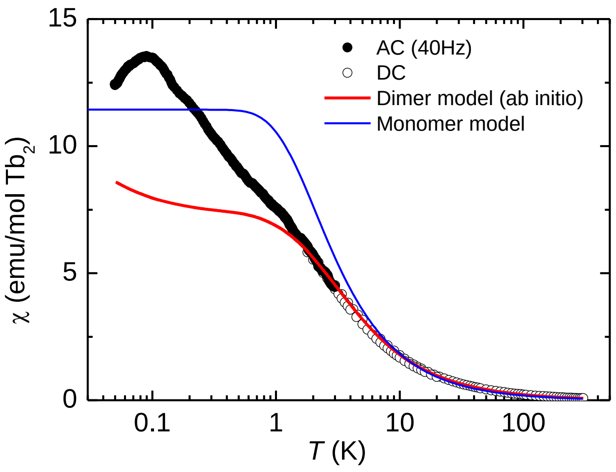

Fig. S3 Susceptibility *vs.* temperature measured by SQUID in DC (open symbols), and in the Dilution Refrigerator in AC at very low frequency, f=40 Hz (bold symbols); Red line: fit within the Tb_2 dimer Hamiltonian model, with single-ion gap, $\Delta_{Tb} / k_B = 3.22$ K , intradimer interaction $J'^* / k_B = -1.6$ K and hyperfine interaction A^*=0.3 K (in a S^*=1/2 Hamiltonian).

S5. Magnetic relaxation results

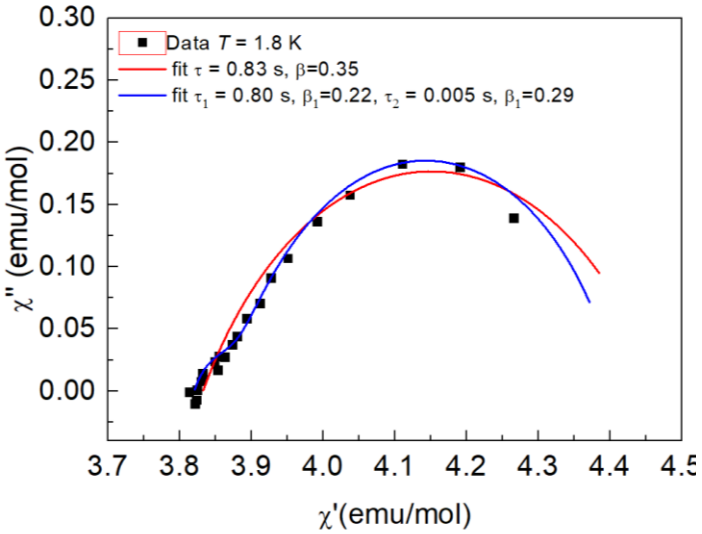

Fig. S4 Cole-Cole plot, $\chi''(\chi')$, at *T*=1.8 K, *H*=4.5 kOe; the data are better fitted by a double-Debye function (blue line) than a single-Debye function (red line), demonstrating the presence of two relaxation processes.

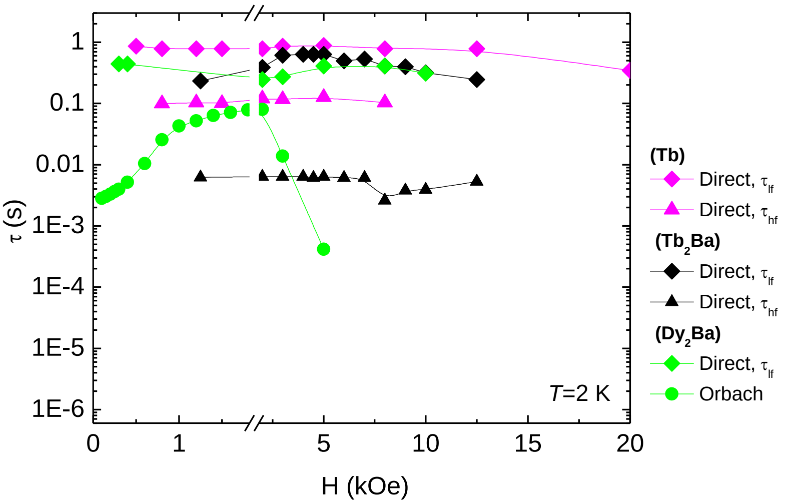

Fig. S5 Relaxation time as a function of the applied fields at *T*=2 K for **(Tb$_2$Ba)** complex (this work), isostructural complex **(Dy$_2$Ba)** and mononuclear complex **(Tb)**.